Nanotechnology **20** (2009) 275602 (10pp) doi:10.1088/0957-4484/20/27/275602

# Dynamics of molecular self-ordering in tetraphenyl porphyrin monolayers on metallic substrates

**Jens Brede[1], Mathieu Linares[2,3], Stefan Kuck[1], Jörg Schwöbel[1], Alessandro Scarfato[1,4], Shih-Hsin Chang[1], Germar Hoffmann[1], Roland Wiesendanger[1], Roy Lensen[5], Paul H J Kouwer[5], Johan Hoogboom[5], Alan E Rowan[5], Martin Bröring[6], Markus Funk[6], Sven Stafström[2], Francesco Zerbetto[7] and Roberto Lazzaroni[3]**

[1] Institute of Applied Physics, University of Hamburg, Jungiusstrasse 9, 20355 Hamburg, Germany
[2] Department of Physics, Chemistry and Biology, Linköping University, 581 83 Linköping, Sweden
[3] Service de Chimie des Matériaux Nouveaux, Université de Mons, 20 Place du Parc, 7000 Mons, Belgium
[4] Dipartimento di Fisica 'E R Caianiello', Università degli Studi di Salerno, Via S Allende, 84081 Baronissi (SA), Italy
[5] Institute for Molecules and Materials, Radboud University, Heyendaalseweg 135, 6525 AJ Nijmegen, The Netherlands
[6] Fachbereich Chemie, Philipps-University Marburg, Hans-Meerwein-Straße, 35032 Marburg, Germany
[7] Dipartimento di Chimica G Ciamician, Università di Bologna, Via F Selmi 2, 40126 Bologna, Italy

E-mail: ghoffman@physnet.uni-hamburg.de

Received 26 February 2009, in final form 25 April 2009
Published 17 June 2009
Online at stacks.iop.org/Nano/20/275602

**Abstract**
A molecular model system of tetraphenyl porphyrins (TPP) adsorbed on metallic substrates is systematically investigated within a joint scanning tunnelling microscopy/molecular modelling approach. The molecular conformation of TPP molecules, their adsorption on a gold surface and the growth of highly ordered TPP islands are modelled with a combination of density functional theory and dynamic force field methods. The results indicate a subtle interplay between different contributions. The molecule–substrate interaction causes a bending of the porphyrin core which also determines the relative orientations of phenyl legs attached to the core. A major consequence of this is a characteristic (and energetically most favourable) arrangement of molecules within self-assembled molecular clusters; the phenyl legs of adjacent molecules are not aligned parallel to each other (often denoted as $\pi$–$\pi$ stacking) but perpendicularly in a T-shaped arrangement. The results of the simulations are fully consistent with the scanning tunnelling microscopy observations, in terms of the symmetries of individual molecules, orientation and relative alignment of molecules in the self-assembled clusters.

M This article features online multimedia enhancements

(Some figures in this article are in colour only in the electronic version)

 

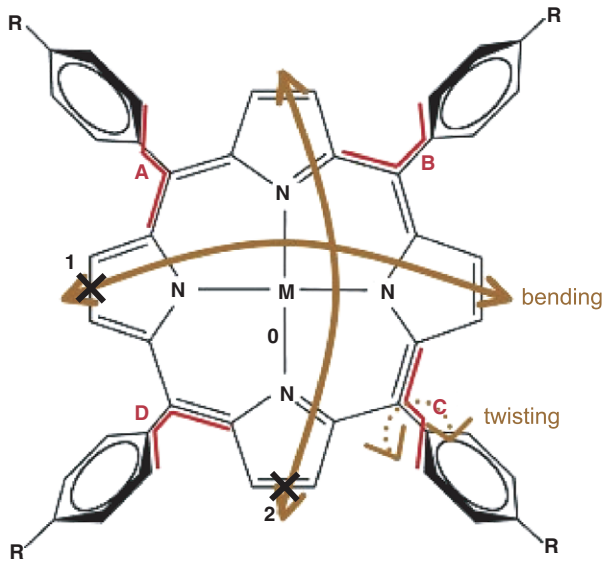


**Figure 1.** Chemical structure of TPP. The molecules have an inner porphyrin core which hosts a metallic centre (M = Co, Cu) or two hydrogen atoms. The porphyrin core can be planar or bent in a saddle conformation. Attached to the core are phenyl rings, which are terminated by H or by an additional substituent R (R = MeS or Br). These phenyl rings are rotatable along their axes. '0','1' and '2' denote positions in the porphyrin core that are relevant for the discussion of the results of molecular modelling.

## 1. Introduction

An important goal in future nanoelectronics is the miniaturization of electronic circuits and other electronic elements to molecular sizes. Besides the reduction in size, usage of single molecules as isolated functional entities gains potentially from a rational design by synthetic means [1]. It is hoped that this approach may lead to advanced opportunities in steering the growth behaviour and other physical properties of molecular assemblies. To this end, however, a detailed understanding of the interaction of such molecules among each other and with their surroundings is of utter importance. This is particularly true for the influence of the substrate on the conformational and electronic properties of a given molecular system.

Due to their extended $\pi$-systems and flat architectures, polyenic and aromatic compounds have often been studied as molecular layers on metallic surfaces. Within this class, porphyrins and metalloporphyrins are preferentially investigated; as these compounds are very robust, poly-functional, volatile and readily available with a range of different electronic and steric properties. Specific questions of modern physics can therefore be addressed by investigating monolayers of tailor-made porphyrins deposited on a solid substrate. Evidence has been provided by local experiments such as scanning tunnelling microscopy (STM) and volume averaging techniques such as near-edge x-ray absorption fine structure spectroscopy that indeed the molecular conformation of porphyrins on metallic substrates deviates from their known shapes in bulk systems [2–4].

The general chemical structure of tetraphenyl porphyrin (TPP) molecules is shown in figure 1. TPP molecules have a porphyrin core with a fourfold symmetry. The centre can host two hydrogen atoms or a metallic ion. The oxidation state, reactivity and electronic properties of the porphyrin moiety are relevant for many biological functions in enzymes as well as oxygen transport in the blood [5]. The four phenyl legs are connected to the porphyrin core via C–C bonds, which allow for rotation and can result in a reduction of symmetry. The crystalline structure of TPP compounds in the bulk has been known for decades. Depending on the metallic centre and the ligand sphere, different deformations of the porphyrin core are reported as ruffled or saddled structures [2, 6, 7]. In recent years, TPP and related molecules adsorbed on a metallic substrate were the subject of intensive local investigations by means of STM [8–11], scanning tunnelling spectroscopy [9, 12–14], STM-assisted manipulation [15–18], STM-induced light emission [19–21] and atomic force microscopy [22].

Results of previous studies indicate that the interaction of the phenyl legs with the surface governs the growth of larger molecular complexes. The molecular structure of the phenyl substituents [23, 24] as well as the exact atomic structure underneath [3] have a drastic influence on the adsorption. In contrast, substitution of the $H_2$ centre with metallic ions in the porphyrin core has no influence on the adsorption but only on electronic properties [12, 25]. The electronic (physical) properties of the porphyrin core are highly relevant for chemical reactivity or magnetism [12, 16, 26–29].

Here, we especially address the role of the phenyl legs on the growth behaviour of TPPs: first, the phenyl legs can have interactions with the substrate, which are likely to influence the adsorption energy and molecular orientation. This in turn can affect the molecular diffusion on the surface. Finally, specific intermolecular interactions between those groups can deeply modify the molecular packing. Adsorption and formation of molecular aggregates are locally studied by means of STM on Cu(111) and Au(111). In contrast to previous studies where self-assembling was observed [12, 30] here TPP molecules are systematically modified. Molecule–molecule interactions are controlled by the chemical synthesis. Experimental results are combined with molecular modelling simulations, to address the underlying dynamic processes present at the first stages of growth, in relation to the nature of the molecule–molecule and molecule–surface interactions.

## 2. Experimental details

### *2.1. Synthesis*

In this work four different TPPs were synthesized under Adler conditions using pyrrole and the corresponding aldehyde [31, 32]. The TPPs were also metallated with cobalt and copper using established procedures [33].

Attempts to isolate 5,10,15,20-tetrakis-(4-methylsulfanyl-phenyl)-porphyrin ($(MeS)_4$TPP) using the procedure by Drain and Gong [34] were unsuccessful. We found that the porphyrin remained on top of the silica during purification by column

chromatography (eluent: $CHCl_3$) as a bright purple compound, and that all the side products were eluted. This allowed us to remove the impurities using a silica plug; after which the pure compound was removed from the plug by Soxhlet extraction for five days in $CH_2Cl_2$ in 14% yield.

*Materials:* unless stated otherwise, all solvents were used without further purification. Silica gel (0.040–0.063 mesh, Silicycle) was used for column chromatography.

*Methods*: (TPP) 5,10,15,20-tetrakis-(phenyl)-porphyrin: benzaldehyde (17.7 g, 167 mmol) was added to a stirring solution of boiling propionic acid (0.5 l). After 5 min, freshly distilled pyrrole (11.6 ml, 167 mmol) was slowly added and the reaction mixture was refluxed for another 2 h. The propionic acid was then removed through evaporation under reduced pressure; after which the black residue was dissolved in 250 ml chloroform. The resulting solution was washed twice with 100 ml 0.1 M NaOH and two portions of water (100 ml), followed by precipitation (twice) in 400 ml methanol. The precipitate was then redissolved in $CHCl_3$ and subjected to column chromatography (eluent: $CHCl_3$), yielding 1.83 g (7%) of TPP. The title compound was further purified by recrystallization from $CH_2Cl_2$. $^1$H-NMR (400 MHz, $CDCl_3$, $\delta$ (ppm)) 8.85 (8H, s, pyrrole H), 8.24 (8H, m, Ar–H), 7.77 (12H, m, Ar–H), −2.76 (2H, s, NH); $^{13}$C-NMR (300 MHz, $CDCl_3$, $\delta$): 142.2, 134.6, 131.0, 127.7, 126.7, 120.1; UV–vis ($CH_2C_l2$) $\lambda$/nm ($\log \epsilon/M^{-1}\ cm^{-1}$): 417 (5.7), 514 (4.3), 549 (3.9), 590 (3.7), 646 (3.7); ESI-MS: $m/z$ calculated for $C_{44}H_{31}N_4$ [M + H]: 615.2549, found: 615.2548.

(Co-TPP) Cobalt-5,10,15,20-tetrakis-(phenyl)-porphyrin: to a stirring solution of refluxing DMF (15 ml) under argon, a small amount of 5,10,15,20-tetrakis-(phenyl)-porphyrin (100 mg, 0.16 mmol) was added. After 5 min, 115 mg (0.46 mmol) of $Co(OAc)_2 * 4H_2O$ was added. The reaction was stopped after 10 min by evaporating the DMF under reduced pressure using a rotary evaporator. The resulting orange solid was redissolved in chloroform and subjected to column chromatography (eluent: $CHCl_3$), yielding 50 mg (46%) of the title compound. IR ($cm^{-1}$): 3452, 2916, 2849, 1725, 1467, 1441, 1349, 1242, 1190, 1004, 795, 749, 702, 610; UV–vis ($CH_2Cl_2$) $\delta$/nm ($\log \varepsilon/M^{-1}\ cm^{-1}$): 411 (5.4), 529 (4.1); ESI-MS: $m/z$ calculated for $C_{44}H_{28}CoN_4$: 671.1646, found: 671.1633.

(Cu-TPP) Copper-5,10,15,20-tetrakis-(phenyl)-porphyrin: a solution of copper(II)acetate monohydrate (160 mg, 0.8 mmol) in methanol (10 ml) was added to 5,10,15,20-tetrakis-(phenyl)-porphyrin (100 mg, 0.16 mmol) in chloroform (10 ml) and the resulting slurry was heated for 10 min. The solvent was removed *in vacuo*, the dark solid redissolved in chloroform and filtered through a plug of silica. The title compound (95 mg, 88%) was obtained after evaporation as a dark violet solid. IR ($cm^{-1}$): 2919, 2852, 1598, 1576, 1440, 1345, 1205, 1177, 1004; UV–vis ($CH_2Cl_2$)/nm ($\log /M^{-1}\ cm^{-1}$): 421 (4.7), 542 (4.3); ESI-MS: $m/z$ calculated for $C_{44}H_{28}CuN_4$: 675.1610, found: 675.1606.

(TBrPP) 5,10,15,20-tetrakis-(4-bromophenyl)-porphyrin: 4-bromobenzaldehyde (1.85 g, 10 mmol) was added to a stirring solution of refluxing propionic acid (50 ml). After 5 min, freshly distilled pyrrole (0.7 ml, 10 mmol) was slowly added and the reaction mixture was refluxed for another 30 min. The same work-up procedure was used as described for TPP and the crystalline material was then redissolved in chloroform and subjected two times to column chromatography (eluent: $CHCl_3$/heptane = 80/20 v/v%), affording 201 mg (9%) of the title compound (rf = 0.88 in toluene/heptane = 70/30 v/v%). $^1$H-NMR (400 MHz, CDCl3, $\delta$ (ppm)) 8.84 (8H, s, pyrrole H), 8.07 (8H, m, Ar–H), 7.90 (8H, m, p-BrAr–H), −2.87 (2H, s, NH); $^{13}$C-NMR (300 MHz, $CDCl_3$, $\delta$): 140.8, 135.8, 131.1, 130.0, 122.6, 119.0; IR ($cm^{-1}$): 3317, 2920, 2850, 1584, 1554, 1472, 1390, 1346, 1070, 1009, 962, 906, 798, 728, 612; ESI-MS: $m/z$ calculated for $C_{44}H_{26}Br_4N_4$ [M + H]: 930.8928, found: 930.8843.

(Co-TBrPP) Cobalt-5,10,15,20-tetrakis-(4-bromophenyl)-porphyrin: the title compound was prepared using the same procedure as Co-TPP and purified using column chromatography (eluent: $CHCl_3$), yielding 64.8 mg (72%) of the title compound. UV–vis ($CH_2Cl_2$) $\delta$/nm ($\log \varepsilon/M^{-1}\ cm^{-1}$): 411 (5.2), 528 (4.0); ESI-MS: $m/z$ calculated for $C_{44}H_{24}Br_4CoN_4$: 982.8067, found: 986.8109.

($(MeS)_4$TPP) 5,10,15,20-tetrakis-(4-methylsulfanyl-phenyl)-porphyrin 4-methylsulfanyl-benzaldehyde (2.66 ml, 20 mmol) was added to a stirring solution of boiling propionic acid (100 ml). After 5 min, freshly distilled pyrrole (1.39 ml, 20 mmol) was slowly added and the reaction mixture was refluxed for another 30 min. After removal of propionic acid under reduced pressure, the black content was dissolved in 100 ml $CH_2Cl_2$ and extracted two times with 100 ml 0.1 M NaOH. The organic layer was then filtered through a small plug of silica using $CH_2Cl_2$, removing all unwanted side products. The title compound remained on top of the silica and was removed. The purple product was then purified by Soxhlet extraction for 5 days using $CH_2Cl_2$. After removal of the solvent under reduced pressure, the product was isolated as a purple solid in 553 mg (14%). No $^{13}$C-NMR was obtained, because of the poor solubility in organic solvents. $^1$H-NMR (400 MHz, $CDCl_3$, $\delta$) 8.87 (8H, m, pyrrole H), 8.13 (8H, m, Ar–H), 7.63 (8H, m, Ar–H), 2.76 (12H, s, $CH_3$), −2.78 (2H, br s, NH). IR ($cm^{-1}$): 3645, 3319, 2954, 2868, 1732, 1470, 1431, 1230, 1159, 1092, 801. UV–vis (THF) $\delta$/nm ($\log \varepsilon/M^{-1}\ cm^{-1}$): 422 (5.6), 517 (4.2), 554 (4.1), 595 (3.7), 652 (3.8); ESI-MS: $m/z$ calculated for $C_{48}H_{39}N_4S_4$ [M + H]: 799.2058, found: 799.2045.

### 2.2. Experimental conditions

Sample preparation and local investigations were performed under ultra-high vacuum conditions ($<2 \times 10^{-10}$ mbar); after introduction into the vacuum system via home-built molecule evaporators, the molecular samples were first degassed for several hours below their sublimation temperatures; then their sublimation rates were determined by means of a quartz microbalance. After preparation of Cu(111) and Au(111) surfaces by standard techniques (several consecutive cycles of argon ion etching and following annealing above 700 K) molecules were deposited on these surfaces. For the study of an isolated molecule, deposition took place with the sample kept at approximately 30 K. Self-assembled molecular clusters were

generated by heating these samples up to room temperature to enable thermally induced mobility. As reference, molecules were also deposited with the sample maintained at room temperature during deposition. After preparation, these samples were locally investigated in a home-built variable-temperature STM operated at approximately 25 K [35]. As local probes for imaging, chemically etched tungsten tips were used. The exact tunnelling parameters are listed in the appendix with $U$ defined as the applied voltage between the STM tip and the sample. Positive voltages refer to tunnelling into unoccupied sample states and negative voltages to tunnelling out of occupied sample states, respectively. All images are processed with WSxM in terms of line and plane fitting procedures [36].

### *2.3. Modelling*

Modelling TPP molecules is based on a two-step approach. First, a conformational study of an isolated molecule by density functional theory (DFT) was performed with the B3LYP/6-31+G(d) formalism. The DFT calculations provide an accurate description of the molecular properties, which is a prerequisite for this work. However, such a theoretical approach cannot be used to represent the intermolecular interactions. For this purpose, the second step of the modelling study, aimed at investigating the adsorption of a single molecule and self-assembly on gold, is based on a force field molecular mechanics and molecular dynamics approach [37, 38]. In this method, the interactions between gold atoms are represented within the Glue model approximation [39]. The dynamics of molecule–molecule interactions are described by MM3 force field calculations [40, 41]. For gold–molecule interactions, a charge equilibration procedure [42] in combination with a repulsive potential is used [43]. This method has already been applied to various systems [44–46] for which the experimental adsorption energies were reproduced with an accuracy better than 1 kcal mol$^{-1}$.

For modelling the adsorption of a single molecule on gold, the molecule was adsorbed on a surface made of four layers of gold; each layer consisting of $14 \times 16$ atoms. The atoms in the top two layers of the surface were allowed to relax while the atoms in the two bottom layers were kept fixed. To simulate an infinite surface, periodic boundary conditions were employed. Considering the size of the cell ($\sim$40.4 Å $\times$ 40 Å) and the cutoff used (9.5 Å), there is no interaction between a single molecule adsorbed on the gold surface and its image in the neighbouring cell.

Then, starting with a molecule optimized on a surface with fourfold rotational symmetry and planar porphyrin core (see figure 4(1)) which is distinctively different to the experimentally observed geometry (twofold mirror symmetry and saddled porphyrin core) we performed molecular dynamics (MD) simulations. The simulations of the dynamic behaviour were carried out within the canonical ensemble, i.e. at a constant number of molecules, volume and temperature (constant $NVT$). All simulations of the dynamic behaviour were realized at 300 K. This reflects the experimental conditions where the formation of molecular clusters is temperature-driven. The temperature is maintained during the dynamics using the Groningen method of coupling to external baths [47]. During the MD simulation of the single molecule adsorbed on the surface, the evolution of the tilting of phenyl legs and bending of the core of the porphyrin were followed and recorded over a period of 100 ps. Based on the adsorption geometry obtained for a single molecule, the self-assembly of four porphyrin molecules deposited on a surface of four layers of $11 \times 12$ atoms of gold was modelled. Such a size was chosen for the unit cell so as to be consistent with the experimental data for the adsorbed molecular layer, while maintaining the computational effort to a tractable level. Again, the two top layers were free to relax, the bottom layers remained fixed, and periodic boundary conditions simulated an infinite monolayer. After an equilibration time of 100 ps in the canonical ensemble, the lattice parameters were followed and recorded for 100 ps.

## 3. Results

### *3.1. Molecular appearance at low coverage*

To learn about the appearance of the different TPPs, STM imaging of isolated molecules, as prepared on a Cu(111) and a Au(111) surface, was performed. Figures 2(a)–(f) show representative STM images. During the preparation and all stages of experiments, thermally induced mobility was prevented by maintaining a continuous cooling below 30 K. The molecules (Cu-TPP, Co-TPP, Co-TBrPP and $(MeS)_4$TPP) show a twofold $C_{2v}$ symmetry with four pronounced lobes. Following [23], these lobes are interpreted as tilted phenyl legs whereas the reduced symmetry of the porphyrin core (in comparison to the structural model) originates from a bending into a saddle conformation. As the appearance of molecules is independent of their orientation on the surface tip artefacts (which might be responsible) can be excluded.

In direct comparison, Cu-TPP and Co-TPP can be distinguished at the given voltage by the characteristic appearance of the centres [48]. Cu-TPP shows a depression whereas Co-TPP a broad protrusion as originating from 3d states of the central ion [12, 49, 50]. Co-TPP and Co-TBrPP significantly vary in the extension of phenyl legs due to attached bromine atoms (not shown, see also [16, 17]). Similarly, $(MeS)_4$TPP, which is for the first time investigated by a local technique, shows the same extension at its phenyl legs as bromine-terminated TPPs whereas again the centre shows a minimum. Due to those differences in their appearances, two or more molecular species on the same surface are easily distinguished. Figure 2(d) presents such a surface with Cu-TPP and Co-TPP deposited on Cu(111).

Comparing adsorption on different surfaces, i.e. on Cu(111) and on Au(111), reveals the role of the substrate on the adsorption geometry. The contrast within molecules remains unaffected whereas the shape can vary drastically. The influence of the substrate is most pronounced for $(MeS)_4$TPP. In STM images of $(MeS)_4$TPP (see figures 2(c) and (f)) the aspect ratio of the short molecular side versus the long molecular side is approximately 1:1.8 on Cu(111) whereas on Au(111) the same ratio is approximately 1:1.1, in line

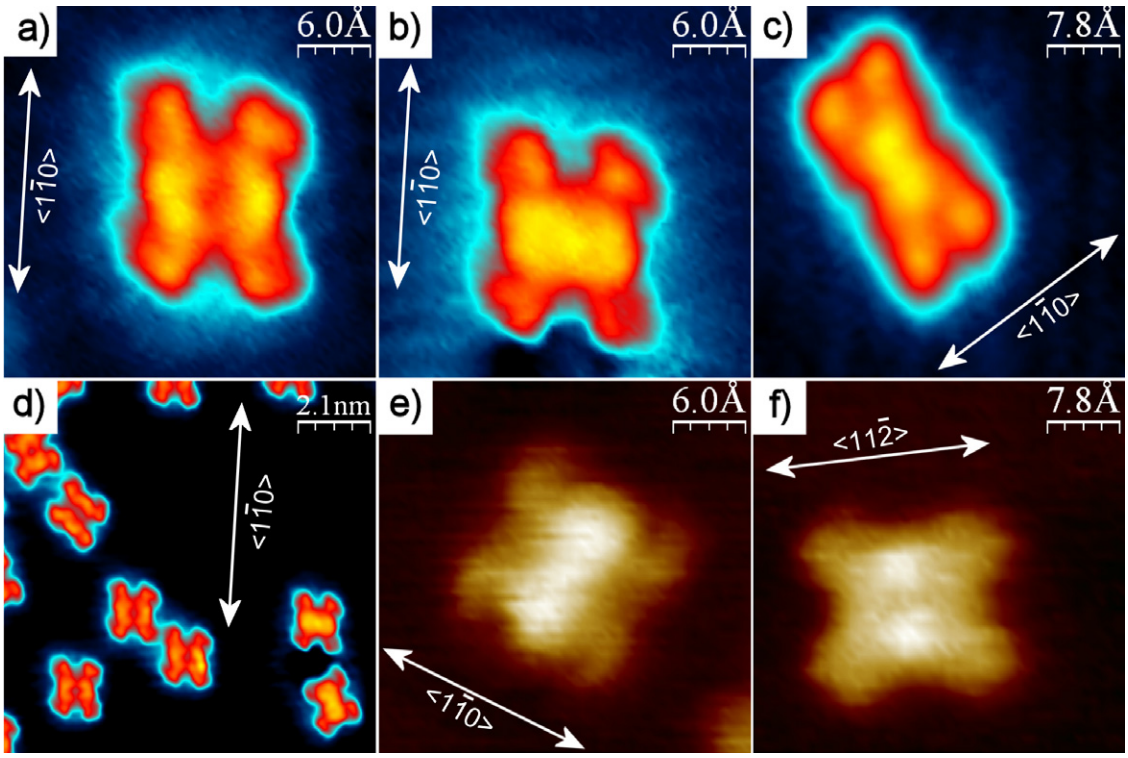


**Figure 2.** High-resolution images of three different and isolated porphyrin molecules for negative voltages on Cu(111) (a)–(d) and on Au(111) ((e) and (f)). (a) shows Cu-TPP, (b) and (e) show Co-TPP and (c) and (f) $(MeS)_4$TPP. The characteristic contrast at the central position and of the four lobes enables a precise identification within mixed samples of Co-TPP and Cu-TPP on Cu(111) as presented in (d). For Cu-TPP and Co-TPP three well-defined orientations are identified, which coincide with the atomic structure underneath.

with [16]. This indicates enhanced sensitivity of the sulfur-terminated ends towards the surface compared to the case of hydrogen termination. Sulfur is known to undergo a strong binding to a gold surface [51]. Sulfur-terminated molecules are established for the formation of self-assembled chemisorbed monolayers from wet solutions [52]. Here, $(MeS)_4$TPP molecules have been designed to clip the end of the phenyl group to the gold surface (as discussed in section 3.4). The origin of the behaviour on different substrates remains speculative as it will reflect a complex interplay of preferred adsorption sites for sulfur and the whole molecule.

We attribute the appearance of $(MeS)_4$TPP to a bending of the in-plane angle between the phenyl groups and the porphyrin core. Moreover, only a few and substrate-specific orientations relative to the crystallographic axes are found for the different TPP molecules [53]. Both observations indicate an adsorption of molecules that is controlled through the interaction of the phenyl groups with the substrate [54].

### *3.2. Formation of long-range ordered molecular clusters*

Deposition of molecules at room temperature or alternatively post-annealing of samples after low-temperature preparation lead to the formation of molecular islands. Several combinations of TPP molecules and substrates were tested on their growth behaviour. Among these, three representative examples are presented in figure 3; Co-TBrPP/Cu(111) in figure 3(a), a mixture of Co-TPP and Cu-TPP on Au(111) in figure 3(b) with the herringbone reconstruction of the substrate impinged into the organic layer, and Cu-TPP/Cu(111) in figure 3(c). All these molecule–substrate systems show a peculiar molecular alignment with high periodicity. The analysis of larger surface areas (not shown) reveals three distinct orientations of molecular domains. This observation reflects that the formation of larger islands is guided by the interaction of molecules with the threefold symmetric substrates.

Within the sensitivity of the experimental conditions, molecular meshes solely formed by Co-TPP (see figure 8(a)) or Cu-TPP on Au(111), and mixed samples of Co-TPP and Cu-TPP on Au(111), are identical in terms of their unit cells and their orientations (and will later be discussed in direct comparison with the numerical results). Additional substituents such as bromine influence the molecular unit cells. This stresses the major influence of the phenyl legs on the growth, whereas the effect of the metallic centre on the growth is negligible.

To study the role and the relative orientation of the phenyl legs, figure 3(c) shows a high-resolution image of Cu-TPP grown on Cu(111). The voltage was chosen so that improved intramolecular contrast was achieved [48]. One peripheral molecule with a clearly resolved structure was selected as reference for analysis of the complex structure within the island. In agreement with the study of isolated TPP molecules this molecule at the edge of the island has a characteristic twofold mirror symmetry. The copper ion in the porphyrin centre results in the characteristic depression of Cu-TPP (see

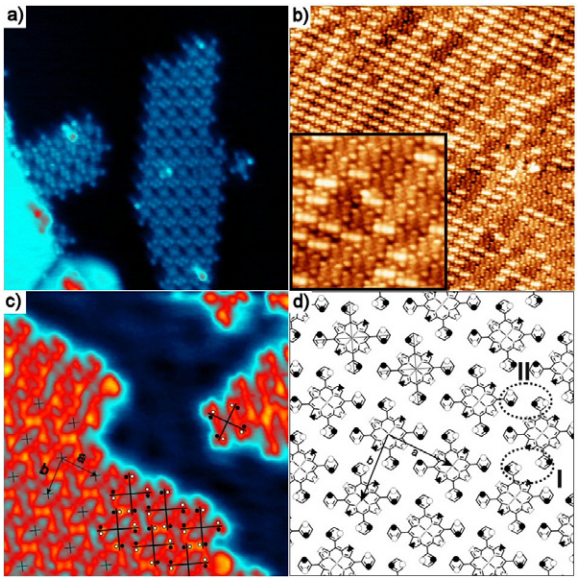


**Figure 3.** (a)–(c) Upon deposition or post-annealing at room temperature hydrogen-and bromine-terminated metallic TPPs show a strong tendency to form well-ordered molecular islands on Cu(111) and Au(111) in STM images. (a) shows an aggregate of Co-TBrPP on Cu(111). In (b) a STM image after room temperature deposition of Co-TPP and Cu-TPP on an Au(111) surface is presented. The resulting structure is intermixed but well ordered, with Co-TPP molecules showing the typical protrusion in the centre. The herringbone reconstruction of the Au(111) surface is transmitted through the organic layer. (c) shows a detailed view into the structure of a Cu-TPP island. For orientation, the centre of each molecule is marked ($x$). Tilting of phenyl legs is indicated by ○ and ● as deduced from a molecule at the edge of a cluster with its internal structure well resolved. (d) depicts the proposed molecular alignment resulting from the analysis of the island. Phenyl legs next to each other are always perpendicularly arranged (indicated by circles I and II). The connecting lines between two opposing ends (△ and ▲, respectively) mark mirror axes of the porphyrin core (Co-TBrPP/Cu(111): $a = 1.70 \pm 0.10$ nm, $b = 1.50 \pm 0.10$ nm, $\angle_{ab} = 83° \pm 5°$; Co-TPP and Cu-TPP/Au(111): $a = 1.45 \pm 0.05$ nm, $b = 1.40 \pm 0.05$ nm, $\angle_{ab} = 87° \pm 3°$; Cu-TPP/Cu(111): $a = 1.29 \pm 0.05$ nm, $b = 1.36 \pm 0.05$ nm, $\angle_{ab} = 80° \pm 5°$).

also figure 2(a)). Tilting of each phenyl group is marked by a ○ and a ● for the lower and the upper sides, i.e., for the side of the phenyl group oriented towards the surface and away from the surface, respectively. Phenyl legs are tilted on an absolute scale by an equal angle as manifested in the observed symmetry whereas the value of the angle cannot be determined from STM images. Phenyl legs opposite to each other are rotated clockwise, the others anti-clockwise (see also figure 6(B) of the later discussion).

The symmetry of single TPPs is periodically reproduced throughout the molecular island. This indicates self-recognition of molecules in identical orientation and adsorption geometry with symmetrically tilted phenyl legs. This is depicted in figure 3(c) which is superimposed by the symbols for the centre and for the two sides of the phenyl legs. With relative positions of the centre and the four phenyl lobes determined, a molecular structure can be deduced (see figure 3(d)). In this structure, none of the phenyl legs that are nearest from one molecule to the next are parallel aligned. Parallel alignment would indicate a $\pi$–$\pi$ stacking, which can be hereby excluded for further interpretation. Instead, nearest neighbours for each phenyl group are perpendicularly oriented; one in terms of the plane of the phenyl lobes (figure 3(d)—I) and the other in terms of the axes of the phenyl lobes (figure 3(d)—II). Similar structures of self-assembled molecular clusters of TPP molecules and derivatives are reported but the underlying physics remained unresolved [30]. The case of pyridyl-terminated porphyrins [12], which was also addressed by force field calculation, is distinctively different as the numerical and experimental results suggest $\pi$–$\pi$ stacking.

In summary, Cu-TPP, Co-TPP and Co-TBrPP adsorbed on Cu(111) and Au(111) form regular networks. The structure of these networks is unaffected by an exchange of the metallic ion whereas modifications of the phenyl groups does alter the unit cell sizes. The unit cell consists of one molecule each with the molecule in a twofold symmetric adsorption geometry. The observed symmetry indicates alternation of clockwise and anti-clockwise rotated phenyl groups. With the structure periodically reproduced it can be concluded that pairs of nearest-neighbour phenyl groups are always perpendicularly rotated. This is a direct consequence of the observed symmetry while the previous assignment of direction (○ versus ● and △ versus ▲) is exchangeable.

### *3.3. Modelling the dynamics and the assembly of porphyrin molecules*

From the comparison of the molecular networks found for different porphyrin species it can be concluded that the adsorption of single molecules as well as the formation of molecular clusters are predominantly governed by the (substituted) phenyl legs, rather than the porphyrin core or the metallic centre. Instead, the interaction of phenyl legs with atoms of the substrate system controls the adsorption of single molecules and formation of clusters. To better understand those issues, simulations on the (numerically) simplest case of a metal-free porphyrin ($H_2$-TPP) in interaction with an Au(111) surface have been performed.

First, a single isolated molecule in the gas phase, i.e. without interaction with any other object—a surface or a neighbouring molecule, was studied at the DFT B3LYP/6-31 + G(d) level in order to determine accurately the conformational behaviour. In the global energy minimum (‘2’ in figure 4) the phenyl groups are tilted by 65° relative to the plane of the porphyrin core, in agreement with previous calculations [55]. The porphyrin core remains planar but the fourfold symmetry is broken due to a specific arrangement of the phenyl groups with opposite orientations of neighbouring phenyl groups (structure ‘2’ in figure 4). This results in a $C_{2v}$ symmetry. Other, energetically less favoured conformations are a propeller shape (‘1’ in figure 4) configuration (by about 0.5 kcal mol$^{-1}$) and configuration ‘3’ (in figure 4) where three phenyl groups are parallel oriented and opposite to the fourth phenyl group ($C_1$ symmetry group, by 0.2 kcal mol$^{-1}$).

To pass from one structure to the other, the phenyl rings can pass through two possible transition states. The first

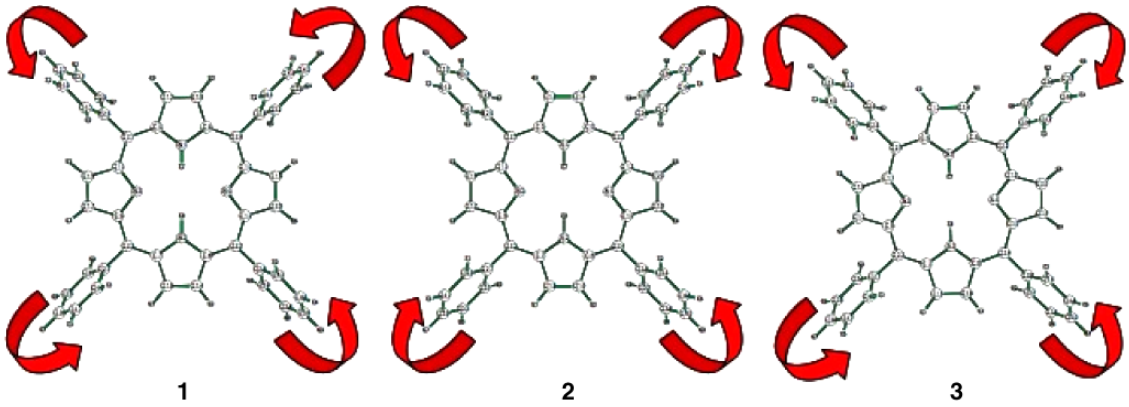


**Figure 4.** Three conformations of TPP in the gas phase related to minima in the potential energy surface. The tilting of phenyl legs is denoted by arrows. Conformation '1' is denoted as propeller shaped within the text. Conformation '2' is the molecule in its global minimum.

transition state has a tilt angle of 90° with a low energy barrier to overcome (0.4 kcal mol$^{-1}$). Passing the other transition state, with a tilt angle of 0° (i.e. with the phenyl ring in the plane of the core), is rather unlikely due to a high transition barrier (16.3 kcal mol$^{-1}$). This high energy barrier of 16.3 kcal mol$^{-1}$ reflects the repulsive interaction between hydrogen atoms in orthopositions of the phenyl ring and hydrogen atoms of the pyrrole ring.

A dynamic simulation of an isolated molecule with the MM3 force field (depicted in figure 5) confirms the DFT results. Indeed the simulation reveals a continuous and uncorrelated rotation of all phenyl legs through 90° at 300 K. This free rotation is expected to be strongly reduced upon adsorption.

The next step was the modelling of the adsorption of a single molecule on an Au(111) surface. In the starting configuration, the TPP molecule is adsorbed in a propeller-shaped configuration on top of gold (see figure 6(A)). The molecule, as well as the first gold layers, are free to relax in the time-dependent simulation.

The time evolution of the tilting of phenyl groups and bending of the porphyrin core is depicted in figure 7. After a short time period of less than 3 ps, the porphyrin rearranges on the surface into a $C_{2v}$ geometry and keeps it during the whole simulation period. The simulation is available as a multimedia enhancement in the online version of the journal at stacks.iop.org/Nano/20/275602. This rearrangement favours the deformation of the core of the porphyrin to increase the adsorption energy on the gold surface. An adsorption energy of $-77.2 \pm 1.3$ kcal mol$^{-1}$ is computed (the adsorption energy is defined as the difference between the energy of the complex (molecule on surface) and the sum of the energies of the molecule and the surface). The final saddle conformation of the molecule after relaxation is illustrated in figure 6(B); in such conformation, the 'back' and 'front' pyrrole rings are tilted with their nitrogen atoms pointing upwards while the 'left' and 'right' pyrrole rings are tilted with their nitrogen atoms closer to the surface. The molecular axis is tilted by 10° relative to the crystallographic axis, with the central position located above a hollow site (see figure 6(C)).

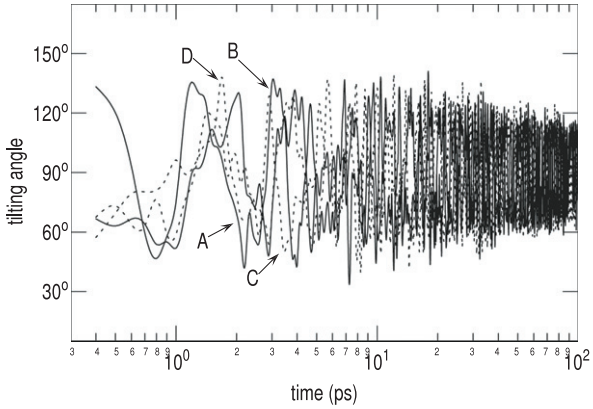


**Figure 5.** Time evolution of tilting angles of the phenyl legs with respect to the plane of the core, at a simulation temperature of 300 K. At this temperature the phenyl legs continuously flip and the TPP porphyrin undergoes transitions between the global minimum (2 in figure 4) and local minima (1 and 3) through 90°.

### *3.4. Comparison of experiment and simulation*

Based on the adsorption geometry obtained for a single molecule, a self-assembly of four porphyrin molecules is built as the elementary structure for a periodic simulation of a full layer and then optimized. The result of this simulation is depicted in figure 8(b). The following lattice parameters are obtained: $a = 1.47 \pm 0.03$ nm, $b = 1.50 \pm 0.02$ nm and an opening angle of $89.0° \pm 1.6°$. Due to the $C_{2v}$ geometry of adsorbed molecules, phenyl rings of adjacent molecules interact in a T-shaped arrangement. It is well known that the most stable configuration for a benzene dimer is the T-shaped conformation, in which the two molecules are perpendicular to each other, with one hydrogen atom of the first molecule pointing to the centre of the $\pi$ system of the second one [56–58]. The presence of a similar conformation here, between phenyl rings of adjacent molecules, indicates the existence of attractive intermolecular interactions which most probably play an important role in the supramolecular organization.

In order to confirm the importance of the orientation of the phenyl groups on the supramolecular organization, the

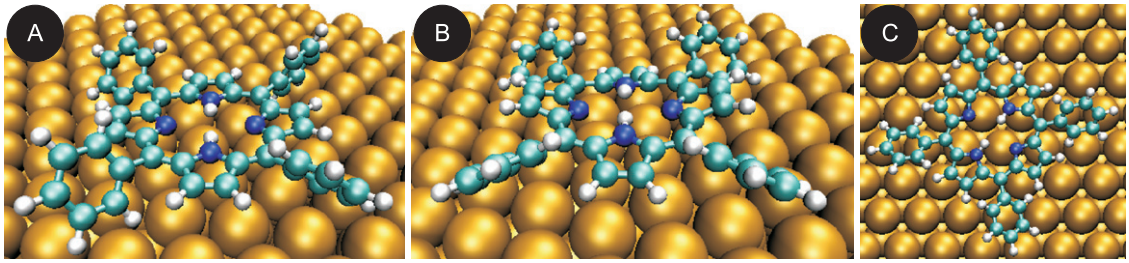


**Figure 6.** (A) shows the initial configuration of the simulation with a TPP molecule in the propeller-shaped conformation. During the course of simulations the porphyrin core bends into a saddle conformation and phenyl legs rearrange. (B) and (C) show the final configuration with the centre of the porphyrin molecule located on top of a hollow site.

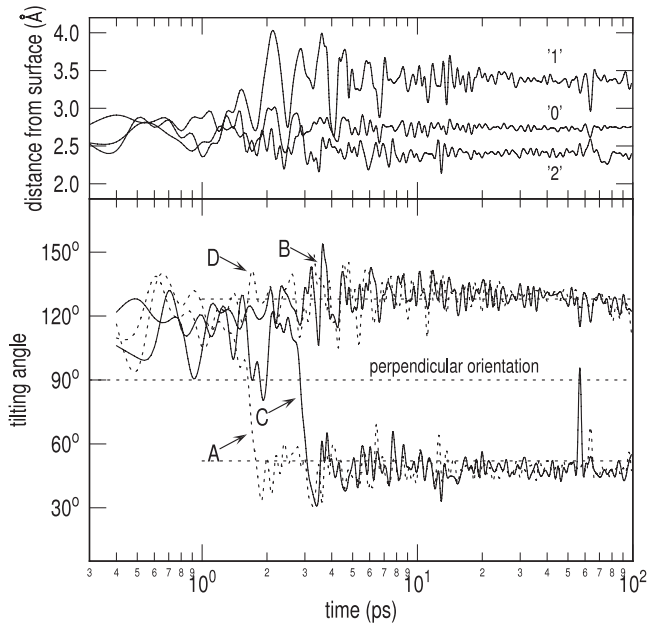


**Figure 7.** Time evolution of $H_2$-TPP adsorption on Au(111). The simulation starts with the molecule in the propeller-shaped geometry. Upper panel: within 3 ps the molecule rearranges into a mirror symmetric conformation with the porphyrin core undergoing a transition into a saddle conformation. This is reflected by the increase of the distance from location '1' and by the decrease of the distance from location '2' relative to the centre of mass denoted as '0'. Positions of '0', '1' and '2' are defined in figure 1. Lower panel: the phenyl legs (A)–(D) align in well-defined orientations relative to the surface plane with the directions alternating relative to the surface normal ($C_{2v}$ symmetry).

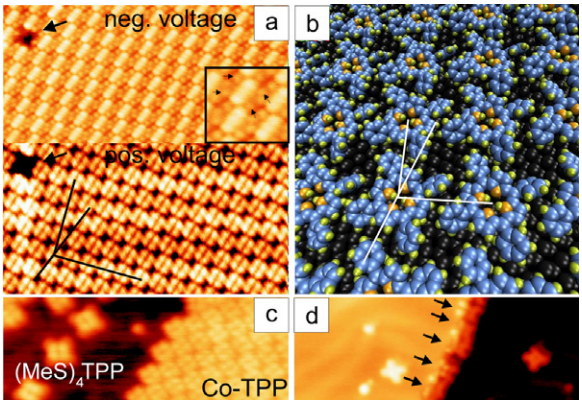


**Figure 8.** Comparison of experimental observations and results from numerical simulations: (a) shows two images of the same Co-TPP island on Au(111) for negative and positive voltage (a defect in the molecular island serves as a marker). The internal molecular structure is clearly resolved. For each molecule protrusions of its four phenyl legs can be identified (see inset) and the molecular axis is tilted relative to the unit cell of the molecular lattice. In agreement, the result of the numerical simulation (b) reflects the same tilting of the molecular axis, the same unit cell, as well as the same arrangement of molecules relative to each other. For orientation, the axes of the unit cell and the molecular axis are indicated. In contrast, (c) and (d) illustrate the role of the phenyl legs for a modified TPP. (c) Whereas Co-TPPs form islands $(MeS)_4$TPP molecules stay isolated when prepared on the same surface in parallel. However, under the given preparation parameters $(MeS)_4$TPP are sufficiently mobile and (d) step edges are fully decorated by $(MeS)_4$TPP.

growth of $(MeS)_4$TPP on Au(111) was compared to Co-TPP. As a consequence of the sulfur termination, the phenyl groups are forced into a (more) planar conformation and thereby suppressing the T-shaped attractive interactions between the phenyl groups on adjacent molecules. This would impede the formation of self-assembled molecular structures. $(MeS)_4$TPP molecules were deposited on the surface at room temperature and studied at 25 K. STM images from this system reveal that self-assembly does not occur (see figures 8(c) and (d)) although under the preparation conditions thermally induced mobility is sufficient for the formation of islands and therefore Au(111) step edges are fully decorated (figure 8(d)).

Then, on top of the same system Co-TPP was deposited at room temperature. Among the isolated $(MeS)_4$TPP molecules well-ordered islands of Co-TPP are formed (figure 8(c)). The two types of molecules can be distinguished by their characteristic appearances in their sizes and their internal structures—here shown when imaging unoccupied molecular states. Figure 8(a) zooms into a region of a large Co-TPP island. For convenience both images as acquired for occupied states (negative voltage) and unoccupied states (positive voltages) are depicted. The unit cell of this island is determined to be $a = 1.45 \pm 0.05$ nm, $b = 1.40 \pm 0.05$ nm and has an opening angle of $87° \pm 3°$. The same unit cell is observed for a mixture of Co-TPP and Cu-TPP/Au(111) as demonstrated in figure 3(b). Individual molecules show a $C_{2v}$ symmetry with the molecular axis tilted by 22° relative to the unit cell. Within the error bar of experimental results we find excellent agreement with the results of the simulation of the self-assembly, as illustrated in figure 8(b).

## 4. Discussion

From the very first stage of molecular growth, a distinct influence of molecule–substrate interaction is present. The preferred orientation of molecules is predefined on highly symmetric surfaces. Adsorption orientation is controlled through the coupling of phenyl legs to the substrate. The influence of the metallic centre in the porphyrin core on the orientation is minor and a decisive influence was not detected experimentally. Additionally, the observed $C_{2v}$ symmetry in STM images suggests an interpretation of a saddle conformation of the porphyrin core. Supporting numerical simulations indicate that this saddle conformation is indeed energetically more favourable than a planar conformation. Due to the presence of a saddle conformation, a thermally stable alignment of phenyl legs is achieved. This is specific to the interaction with the surface since, in the gas phase, bending of the porphyrin core is energetically suppressed and results in a continuous and thermally induced rotation of phenyl legs. The deformation of the porphyrin core results from an attractive interaction between the core and the metallic surface. Although experimentally no evidence for the influence of the metallic ion was found it can be assumed that larger ions than $Co^{2+}$ or $Cu^{2+}$ will cause an inherent stress on the porphyrin core [49] and might lead to a modified adsorption of such a TPP molecule on a surface.

At higher coverage the growth of larger molecular clusters was experimentally observed. Again, the results from STM imaging suggest that not only the adsorption of single TPP molecules, but also the self-assembly process and therefore the interaction of molecules among each other, is driven by the T-shaped interaction of phenyl legs. We calculated this stabilization due to intermolecular interaction between porphyrins at 6 kcal $mol^{-1}$ and per molecule. Modelling of the dynamic behaviour of several molecules in close contact reveals a resulting superstructure which is in perfect agreement with the structure deduced from experimental observations. The calculated superstructure for TPP reflects a complex interplay of different mechanisms; on the one hand, the interaction of TPP molecules with the substrates favours a saddle conformation. This conformation simultaneously predefines the relative orientations of phenyl legs and reduces degrees of freedom for the self-assembling process towards the lowest energy situation. On the other hand, an attractive interaction acts among phenyl legs. However, parallel alignment of phenyl legs, i.e. $\pi$–$\pi$ stacking due to overlap of delocalized $\pi$ electrons, would coincide with a larger steric interaction of phenyl legs with the pyrrole ring of the neighbouring porphyrin core due to the bending of the core. Instead of $\pi$–$\pi$ stacking, T-stacking of phenyl legs is preferred. T-stacking maximizes the area of attractively interacting molecular surface. Similar mechanisms have been proposed for the formation of molecular crystals with a T-stacking arrangement [59, 60]. To experimentally test the influence of the orientation of phenyl legs on the self-assembling process and to suppress T-stacking, the adsorption of hydrogen-terminated TPPs and of $(MeS)_4$TPP was compared. $(MeS)_4$TPP on Cu(111) and Au(111) does not show any tendency of attractive molecule–molecule interaction. This is due to the strong S–Au coupling which forces an in-plane tilting of phenyl legs.

## 5. Conclusion

A systematic study of the growth behaviour of tailor-made tetraphenyl porphyrins adsorbed on Cu(111) and Au(111) is presented by means of STM. Observations are compared to results of DFT calculations and, for the first time, to the numerical simulation of the dynamic behaviour of tetraphenyl porphyrins in the gas phase, of individual molecules in contact with a metallic substrate, and of an assembly of molecules interacting with each other and in direct contact with a metallic surface. The comparison shows excellent qualitative and quantitative agreement. Within molecular clusters, relative orientations of molecules is T-stacking-like. This maximizes the interacting molecular surface and explains similar observations for molecular crystals. Further experimental evidence is given by the intended suppression of self-assembling for the newly introduced $(MeS)_4$TPP due to an increased surface attraction via sulfur termination.

## Acknowledgments

We wish to acknowledge the funding of the EU Project SpiDMe and through the DFG under SFB 668-A5 and GrK 611. The modelling work was supported by the European Commission Marie Curie Research Training Network CHEXTAN (MRTN-CT-2004-512161), by the Interuniversity Attraction Pole Programme of the Belgian Federal Science Policy Office (PAI 6/27), by FNRS-FRFC and by the Swedish Research Council (VR).

## Appendix

Tunnelling parameters:

Figure 2(a) Cu-TPP/Cu(111): $U = -1000$ mV, $I = 50$ pA, $3 \times 3$ nm$^2$.

Figure 2(b) Co-TPP/Cu(111): $U = -1000$ mV, $I = 50$ pA, $3 \times 3$ nm$^2$.

Figure 2(c) $(MeS)_4$TPP/Cu(111): $U = -1000$ mV, $I = 100$ pA, $4 \times 4$ nm$^2$.

Figure 2(d) Co-TPP and Cu-TPP/Cu(111): $U = -1000$ mV, $I = 50$ pA, $10.6 \times 10.6$ nm$^2$.

Figure 2(e) Co-TPP/Au(111): $U = -1200$ mV, $I = 100$ pA, $3 \times 3$ nm$^2$.

Figure 2(f) $(MeS)_4$TPP/Cu(111): $U = -1500$ mV, $I = 100$ nA, $4 \times 4$ nm$^2$.

Figure 3(a) Co-TBrPP/Cu(111): $U = -368$ mV, $I = 166$ pA, $20 \times 20$ nm$^2$.

Figure 3(b) Cu-TPP and Co-TPP/Au(111): $U = -1200$ mV, $I = 100$ pA, $35 \times 35$ nm$^2$.

Figure 3(c) Cu-TPP/Cu(111): $U = 143$ mV, $I = 340$ pA, $10 \times 10$ nm$^2$.

Figure 8(a), (neg. voltage) Co-TPP/Au(111): $U = -1200$ mV, $I = 97$ pA, $10 \times 20$ nm$^2$.

Figure 8(a), (pos. voltage) Co-TPP/Au(111): $U = 2000$ mV, $I = 97$ pA, $10 \times 20$ nm$^2$.

Figure 8(c) Co-TPP and $(MeS)_4$TPP/Au(111): $U = 2000$ mV, $I = 97$ pA, $7 \times 20$ nm$^2$.

Figure 8(d) $(MeS)_4$TPP/Au(111): $U = -1000$ mV, $I = 106$ pA, $10 \times 30$ nm$^2$.

## References


[1] Joachim C, Gimzweski J K and Aviram A 2000 *Nature* **408** 541 and references therein
[2] Fleischer E B, Miller C K and Webb L E 1964 *J. Am. Chem. Soc.* **86** 2342
[3] Jung T A, Schlittler R R and Gimzewski J K 1997 *Nature* **386** 696
[4] Unger E, Beck M, Lipski R J, Dreybrodt W, Medforth C J, Smith K M and Schweitzer-Stenner R 1999 *J. Phys. Chem.* B **103** 10022
[5] Shelnutt J A, Song X-Z, Ma J-G, Jia S-L, Jentzen W and Medforth C J 1998 *Chem. Soc. Rev.* **27** 31
[6] Kosal M E and Suslick K S 1967 *J. Am. Chem. Soc.* **89** 3331
[7] Kosal M E and Suslick K S 2000 *J. Solid State. Chem.* **152** 87
[8] Kunitake M, Batina N and Itaya K 1995 *Langmuir* **11** 2337
[9] Deng W and Hipps K W 2003 *J. Phys. Chem.* B **107** 10738
[10] Hai N T M, Gasparovic B, Wandelt K and Broeckmann P 2007 *Surf. Sci.* **601** 2597
[11] Wintjes N, Bonifazi D, Cheng F, Kiebele A, Stöhr M, Jung T, Spillmann H and Diederich F 2007 *Angew. Chem. Int. Edn* **46** 4089
[12] Auwärter W, Weber-Bargioni A, Brink S, Riemann A, Schiffrin A, Ruben M and Barth J V 2007 *ChemPhysChem* **8** 250
[13] Zotti L A, Teobaldi G, Hofer W A, Auwärter W, Weber-Bargioni A and Barth J V 2007 *Surf. Sci.* **601** 2409
[14] Weber-Bargioni A, Auwärter W, Klappenberger F, Reichert J, Lefrancois S, Strunskus T, Wöll C, Schiffrin A, Pennec Y and Barth J V 2008 *ChemPhysChem* **9** 89
[15] Moresco F, Meyer G, Rieder K H, Tang H, Gourdon A and Joachim C 2001 *Phys. Rev. Lett.* **87** 088302
[16] Iancu V, Deshpande A and Hla S-W 2006 *Nano Lett.* **6** 820
[17] Grill L, Dyer M, Lafferentz L, Persson M, Peters M V and Hecht S 2007 *Nat. Nanotechnol.* **2** 687
[18] Iancu V, Deshpande A and Hla S-W 2007 *Phys. Rev. Lett.* **97** 266603
[19] Qiu X H, Nazin G V and Ho W 2003 *Science* **299** 542
[20] Guo X-L, Dong Z-C, Trifonov A S, Miki K, Mashiko S and Okamoto T 2004 *Nanotechnology* **15** S402
[21] Dong Z-C, Guo X-L, Trifonov A S, Dorozhkin P S, Miki K, Kimura K, Yokoyama S and Mashiko S 2004 *Phys. Rev. Lett.* **92** 086801
[22] Loppacher Ch, Bammerlin M, Guggisberg M, Meyer E, Güntherodt H-J, Lüthi R, Schlittler R and Gimzewski J K 2001 *Appl. Phys.* A **72** S105
[23] Auwärter W, Klappenberger F, Weber-Bargioni A, Schiffrin A, Strunskus T, Wöll Ch, Pennec Y, Riemann A and Barth J V 2007 *J. Am. Chem. Soc.* **129** 11279
[24] Wintjes N, Hornung J, Lobo-Checa J, Voigt T, Samuely T, Thilgen C, Stöhr M, Diederich F and Jung T A 2008 *Chem.—Eur. J.* **14** 5794
[25] Buchner F, Schwald V, Comanici K, Steinrück H-P and Marbach H 2007 *ChemPhysChem* **8** 241
[26] Erler B S, Scholz W F, Lee Y J, Scheidt W R and Reed C A 1987 *J. Am. Chem. Soc.* **109** 2644
[27] Scheybal A, Ramsvika T, Bertschingera R, Puteroa M, Nolting F and Jung T A 2005 *Chem. Phys. Lett.* **411** 214
[28] Wende H *et al* 2007 *Nat. Mater.* **6** 516
[29] Hulsken B, Van Hameren R, Gerritsen J W, Khoury T, Thordarson P, Crossley M J, Rowan A E, Nolte R J M, Elemans J A A W and Speller S 2007 *Nat. Nanotechnol.* **2** 285
[30] Buchner F, Comanici K, Jux N, Steinrück H-P and Marbach H 2007 *J. Phys. Chem.* C **111** 13531
[31] Adler A D, Longo F R, Finarelli J D, Goldmacher J, Assour J and Korsakoff L 1967 *J. Org. Chem.* **32** 476
[32] Martensson J, Sandros K and Wennerstrom O 1994 *J. Phys. Org. Chem.* **7** 534
[33] Fuhrhop J-H and Smith K M 1975 *Porphyrins and Metalloporphyrins* (New York: Elsevier) chapter 19
[34] Drain C M and Gong X 1997 *Chem. Commun.* **21** 2117
[35] Kuck S, Wienhausen J, Hoffmann G and Wiesendanger R 2008 *Rev. Sci. Instrum.* **79** 083903
[36] Horcas I, Fernandez R, Gomez-Rodriguez J M, Colchero J, Gomez-Herrero J and Baro A M 2007 *Rev. Sci. Instrum.* **78** 013705
[37] Baxter R, Teobaldi G and Zerbetto F 2003 *Langmuir* **19** 7335
[38] Teobaldi G and Zerbetto F 2007 *J. Phys. Chem.* C **111** 13879
[39] Ercolessi F, Parrinello M and Tosatti E 1988 *Phil. Mag.* A **58** 213
[40] Allinger N L, Yuh Y H and Lii J-H 1989 *J. Am. Chem. Soc.* **111** 8551
[41] Ma B, Lii J H and Allinger N L 2000 *J. Comput. Chem.* **21** 813
[42] Rappe A K and Goddard W A 1991 *J. Phys. Chem.* **95** 3358
[43] Von Born M and Mayer J E 1933 *Z. Phys.* **75** 1
[44] Montalti M, Prodi L, Zaccheroni N, Baxter R J, Teobaldi G and Zerbetto F 2003 *Langmuir* **19** 5172
[45] Baxter R J, Rudolf P, Teobaldi G and Zerbetto F 2004 *ChemPhysChem* **5** 245
[46] Rapino S and Zerbetto F 2005 *Langmuir* **21** 2512
[47] Berendsen H J C, Postma J P M, van Gunsteren W F, DiNola A and Haak J R 1984 *J. Chem. Phys.* **81** 3684
[48] Scudiero L, Barlow D E and Hipps K W 2000 *J. Phys. Chem.* B **104** 11899
[49] Liao M-S and Scheiner S 2002 *J. Chem. Phys.* **117** 205
[50] Weber-Bargioni A, Reichert J, Seitsonen A P, Auwärter W, Schiffrin A and Barth J V 2008 *J. Phys. Chem.* C **112** 3453
[51] Nuzzo R G, Zegarski B R and Dubois L H 1987 *J. Am. Chem. Soc.* **109** 733
[52] Ulman A 1996 *Chem. Rev.* **96** 1533
[53] Brede J, Linares M, Lensen R, Rowan A E, Funk M, Bröring M, Hoffmann G and Wiesendanger R 2009 *J. Vac. Sci. Technol.* B **27** 799
[54] de Jong M P, Friedlein R, Sorensen S L, Ohrwall G, Osikowics W, Tengsted C, Jonsson S K M, Fahlman M and Salaneck W R 2005 *Phys. Rev.* B **72** 035448
[55] Yokoyama T, Yokoyama S, Kamikado T and Mashiko S 2001 *J. Chem. Phys.* **115** 3814
[56] Hill J G, Platts J A and Werner H-J 2006 *Phys. Chem. Chem. Phys.* **8** 4072
[57] Park Y C and Lee J S 2006 *J. Phys. Chem.* A **110** 5091
[58] Bludský O, Rubeš M, Soldán P and Nachtigall P 2008 *J. Chem. Phys.* **128** 114102
[59] Grimme S 2008 *Angew. Chem. Int. Edn* **47** 3430
[60] Jha P C, Rinkevicius Z, Ågren H, Sealb P and Chakrabarti S 2008 *Phys. Chem. Chem. Phys.* **10** 2715